

## Lung imaging in asthmatic patients: The picture is clearer

Mario Castro, MD, MPH,<sup>a</sup> Sean B. Fain, PhD,<sup>b</sup> Eric A. Hoffman, PhD,<sup>c</sup> David S. Gierada, MD,<sup>a</sup> Serpil C. Erzurum, MD,<sup>d</sup> Sally Wenzel, MD,<sup>e</sup> for the National Heart, Lung, and Blood Institute's Severe Asthma Research Program St Louis, Mo, Madison, Wis, Iowa City, Iowa, Cleveland, Ohio, and Pittsburgh, Pa

**Imaging of the lungs in patients with asthma has evolved dramatically over the last decade with sophisticated techniques, such as computed tomography, magnetic resonance imaging, positron emission tomography, and single photon emission computed tomography. New insights into current and future modalities for imaging in asthmatic patients and their application are discussed to potentially shed a clearer picture of the underlying pathophysiology of asthma, especially severe asthma, and the proposed clinical utility of imaging in patients with this common disease. (J Allergy Clin Immunol 2011;■■■■:■■■■-■■■■.)**

**Key words:** Asthma, imaging, chest computed tomography, magnetic resonance imaging

Imaging of the lungs in patients with asthma has evolved dramatically over the last decade with sophisticated techniques, such as computed tomography (CT), magnetic resonance imaging (MRI), positron emission tomography (PET), and single photon emission computed tomography (SPECT). Previous reports in asthmatic patients have been primarily limited to gross anatomic abnormalities, such as the presence of bronchiectasis, atelectasis, or bronchial wall thickening, which have been noted in asthmatic patients, especially those with severe disease, compared with healthy subjects.<sup>1-3</sup>

Newer imaging techniques are playing an increased role as we seek to assess airway anatomy, regional lung mechanics, and associated lung function (gas exchange) to best understand the

### Abbreviations used

ADC:	Apparent diffusion coefficient
CT:	Computed tomography
EBUS:	Endobronchial ultrasonography
FDG:	Fluorodeoxyglucose
FRC:	Functional residual capacity
HP He:	Hyperpolarized helium
HU:	Hounsfield units
MDCT:	Multidetector-row computed tomography
MRI:	Magnetic resonance imaging
OCT:	Optical coherence tomography
PET:	Positron emission tomography
RV:	Residual volume
SARP:	Severe Asthma Research Program
SPECT:	Single photon emission computed tomography
<sup>99m</sup> Tc-HMPAO:	Technetium <sup>99m</sup> -hexamethylpropylene amine oxime
TLC:	Total lung capacity
WA:	Wall area
WT:	Wall thickness

differences between the lungs of healthy subjects versus those with asthma and to further understand the differences between severe and nonsevere asthma. The respiratory system has both active and passive mechanisms to effectively match the regional flow of fresh gas to the regional flow of mixed venous blood in healthy subjects. These mechanisms result in a system that is complex, involving interactions between the inherent and acquired structural heterogeneity of the bronchial and vascular trees, with feedback systems designed to impose homeostasis, optimizing regional gas exchange. The system ultimately must be examined in the intact dynamic state to understand such complexity and its alterations in asthmatic patients. Such an examination requires both the spatial and temporal resolution necessary to evaluate details of anatomy (airways and parenchyma) and function (regional delivery of gas or blood along with changes in regional lung morphometry or parenchymal density). Furthermore, new imaging modalities are emerging to help us understand the molecular and cellular aspects of lung health and disease.

As these new imaging techniques emerge, clinicians are challenged with understanding the potential clinical benefits these modalities will have for their patients with asthma, as well as the associated risks. In addition, clinical researchers are finding that perhaps imaging can provide a quantitative end point that can be used in intervention studies in asthmatic patients. These new insights into current and future modalities for imaging in asthmatic patients and their application are discussed to potentially shed a clearer picture of the underlying pathophysiology of asthma, especially severe asthma, and the proposed clinical utility of imaging in patients with this common disease.

From <sup>a</sup>the Division of Pulmonary and Critical Care Medicine, Washington University School of Medicine, St Louis; <sup>b</sup>the Department of Medical Physics, University of Wisconsin, Madison; <sup>c</sup>University of Iowa College of Medicine, Iowa City; <sup>d</sup>The Cleveland Clinic Foundation, Cleveland; <sup>e</sup>University of Pittsburgh Medical Center, Pittsburgh.

Supported by National Institutes of Health/National Heart, Lung, and Blood Institute grants HL69149, HL64368, HL69349, HL69170, HL-69155, HL69130, HL69167, HL69116, and HL69174 and the Hartwell Foundation (S.B.F.).

Disclosure of potential conflict of interest: M. Castro is a consultant for Electrocure, NKIT, Schering-Plough, Asthmatx, and Cephalon; is on the advisory board and is a speaker for Genentech; is a speaker for AstraZeneca, Boehringer Ingelheim, Pfizer, Merck, and GlaxoSmithKline; has received royalties from Elsevier; and has received grants from Asthmatx, Amgen, Ception, Genentech, MedImmune, Merck, Novartis, the National Institutes of Health, and GlaxoSmithKline. S. B. Fain is a consultant for and has received research support from GE Healthcare. E. A. Hoffman is a consultant for Roche, Sanofi-Aventis, and Spiration and is a founder and shareholder of VIDA Diagnostics. S. C. Erzurum is owner of Asthmatx. The rest of the authors have declared that they have no conflict of interest.

Received for publication November 6, 2010; revised April 10, 2011; accepted for publication April 18, 2011.

Reprint requests: Mario Castro, MD, MPH, Washington University School of Medicine, Campus Box 8052, 660 S Euclid, St Louis, MO 63110-1093. E-mail: castrom@wustl.edu.

0091-6749/\$36.00

© 2011 American Academy of Allergy, Asthma & Immunology

doi:10.1016/j.jaci.2011.04.051

## STRUCTURE AND FUNCTIONAL IMAGING THROUGH X-RAY CT IN ASTHMATIC PATIENTS

X-ray CT has emerged as the modality of choice for a comprehensive assessment of the lung by allowing for both a detailed assessment of the airway tree, vascular tree, parenchyma, pulmonary blood volume,<sup>4</sup> and regional ventilation.<sup>5-12</sup> Multislice or multidetector-row computed tomography (MDCT) scanner technology involves using multiple detector rings to acquire multiple cross-sectional slices of patients' data with acquisition of the entire lung volume with submillimeter spatial resolution in as little as 0.6 seconds. Faster scan times significantly affect functional imaging protocols in which the rate of delivery of a contrast agent (iodine for perfusion or xenon for ventilation) is measured over time. These faster scan times also minimize the breath-hold time, which is critical when imaging patients with respiratory disease. In fact, with a scan time for the whole lung, it is possible to obtain clinically useful image data without a breath hold, if necessary.<sup>13-21</sup>

### Computer-based quantitation of lung CT images

One problem with CT assessment is that the reproducibility of highly trained readers is at very best around 77% when visual assessment is strictly based on gross pathologic derangement.<sup>22</sup> When the task is defined in terms of what is desired rather than what the human observer can deliver, the interobserver and intra-observer agreements are 30% to 50%. With the goal of using imaging in asthmatic patients to identify homogeneous subphenotypes that can be targeted by new interventions, objective and robust computer-based methods for quantitative assessment of the images have evolved for the lungs, lobes, airways, and vasculature.<sup>23</sup>

### Central airways CT imaging

There has been extensive use of 2-dimensional CT methodologies to evaluate basic airway physiology.<sup>19,24-28</sup> Thinner image slices are desirable to aid in the 3-dimensional analysis of airway tree structure but typically have the cost of a higher radiation dose. In practice one can increase nominal slice thickness from 0.6 to 0.75 mm and reconstruct the slices with slight overlap to achieve adequate signal/noise ratios while keeping the dose in an acceptable range.<sup>20,29</sup> With thinner slice imaging, workers have demonstrated the ability to extract up to 10 generations of the airway tree, and quantitation is achievable out to approximately the sixth generation when slice thickness and in-plane pixel dimensions are minimized.<sup>30-32</sup> Furthermore, by identifying the centerlines of the airway tree, which then define the branch points, it is possible for the computer to automatically identify the airway segments and provide standardized labeling. This process facilitates the comparison of an individual airway segment across lung volumes and over time and allows for clinical research in asthmatic patients to be performed with comparison of similar airway tree structures across patients. Such an automated labeling of the airway tree is demonstrated in Fig 1. By using these methodologies in asthmatic patients, it has been shown that the strongest correlation with airflow limitation is found through airway wall measurements of the more distal airways (fourth to sixth generation).<sup>33-35</sup>

### Parenchymal CT imaging

**Density-based analysis.** Computer-based methods for objective quantitation of CT datasets to compare normal and

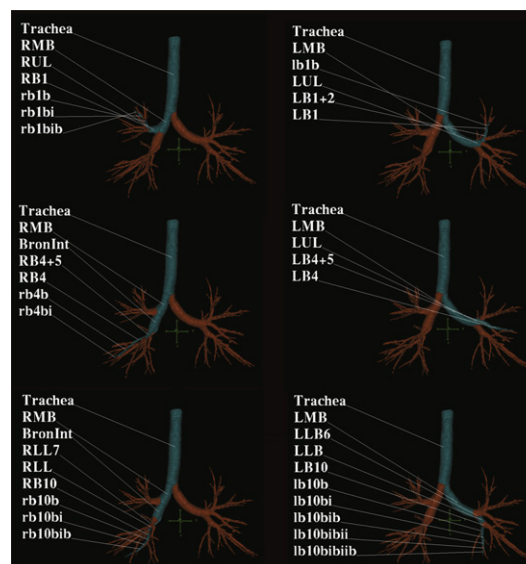


**FIG 1.** Quantitative CT of the airways in asthmatic patients. MDCT analysis was performed with the Pulmonary Workstation software (VIDA, Coralville, Iowa), and a screen capture of the cross-sectional MDCT image is demonstrated across 3 segmental pathways (in blue) in the right and left lungs. *BronInt*, Bronchus intermedius; *LLB*, left lower lobe bronchus; *LMB*, left main bronchus; *LUL*, left upper lobe; *RLl*, right lower lobe; *RMB*, right main bronchus; *RUL*, right upper lobe.

diseased lungs are increasingly being used. Early studies demonstrated that CT density (in Hounsfield units [HU]) is proportional to regional air/tissue ratios.<sup>36</sup> Thus set fixed thresholds of HU can be used to assess regional hyperdistension, emphysema, or air trapping, depending on the lung volume used during scanning. Methods have ranged from the simplest form, which counts the number of voxels at less than a cutoff ( $-900$  HU)<sup>37-48</sup> to those that make use of measures derived from the histogram, including skewness and kurtosis.<sup>49</sup> Critical to the use of lung density to infer the presence and progression of disease is the standardization of the volume at which one images the lung. It is well recognized that lung density measurements change with lung inflation volume. Emphysema-like lung is assessed by coaching the patient to inspire to total lung capacity (TLC). Imaging is accomplished with the patient holding his or her breath at either functional residual capacity (FRC) or residual volume (RV) to assess regional air trapping. Empirically, it has been accepted that voxels decreasing to less than approximately  $-850$  HU are considered to represent trapped lung regions.<sup>50-52</sup> Fig 2 demonstrates the difference between air-trapped regions in a patient with severe and nonsevere asthma. Fig 3 demonstrates the 3-dimensional combination of both quantitative MDCT airway and parenchymal measurements in the same patient.

**Ventilation-based analysis.** The measurement of lung ventilation, lung volume, and tidal volume has traditionally been made for the entire lung, despite the fact that lung function in both health and disease is inhomogeneously distributed throughout the lung.<sup>53-62</sup> Xenon-enhanced CT is a method for the noninvasive measurement of regional pulmonary ventilation determined from the wash-in and washout rates of the radiodense nonradioactive gas xenon, as measured in serial CT scans. Xenon gas has anesthetic properties at concentrations of greater than 30%. Thus for wash-in studies in human subjects, one does not go over this concentration.<sup>63,64</sup> When using xenon-enhanced CT, selection

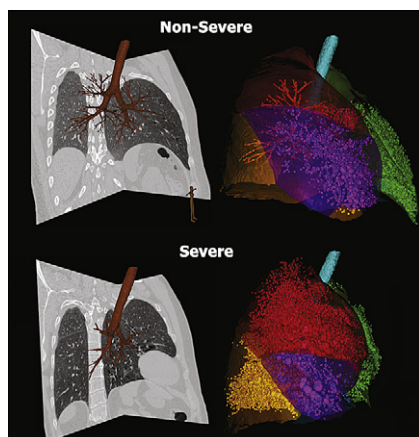


**FIG 2.** Quantitative CT of the lungs in asthmatic patients. Quantitative CT allows accurate assessment of air trapping in asthmatic patients: nonsevere (upper row) and severe asthma (lower row). Trapped air, defined as voxels within the lung field decreasing to less than  $-856$  HU, is demonstrated by spheres proportional to the area of air trapping (volume-rendered view) in the right panels. Each lobe is color-coded. Corresponding CT sagittal views are shown in the left panels. For patients with nonsevere asthma (upper row), the percentage of air trapping ( $<-856$  HU) is as follows: right upper lobe, 3%; right middle lobe, 17%; right lower lobe, 0.5%; left upper lobe, 6%; and left lower lobe, 8%. For patients with severe asthma (lower row), the percentage of air trapping ( $<-856$  HU) is as follows: right upper lobe, 28%; right middle lobe, 60%; right lower lobe, 29%; left upper lobe, 25%; and left lower lobe, 27%.

of normalization factors is important in applying physiological interpretations to the data.<sup>65-69</sup> Ventilation, for instance, can be normalized to regional air content, tissue content, or simply as a mean normalized value. One can achieve approximately 2.5 HU contrast enhancement per percentage of xenon gas, and thus the xenon signal amounts to approximately 50 or 60 HU. This can be enhanced by adding krypton to the gas mixture.<sup>68</sup> Krypton is more inert than xenon but has less radio-opacity than xenon gas. Thus it is not suitable for use on its own but can be used to enhance the xenon signal above that achievable when one is limited to a 30% concentration of xenon.<sup>70-74</sup>

**Perfusion-based analysis.** Dynamic imaging methods, such as CT, have provided access to temporal signals from the vasculature of the lungs that have been used to estimate arterial, venous, and capillary transit times and capillary flow distributions.<sup>75-78</sup> While imaging a patient during a breath hold, a sharp bolus of iodinated contrast agent is injected, and images are acquired and gated to the electrocardiogram. Temporal sequences provide the timing of the passage of the iodine through the lung parenchyma. By comparing the peak of the parenchymal curve with the area under the arterial curve, one achieves a quantitative measure of parenchymal perfusion. As application of imaging modalities to the study of lung disease has progressed, it has become clear that one must begin to evaluate regional lung function and not just an anatomic road map if one is to best use imaging to understand the basis for observed patterns of pathology.<sup>79,80</sup>

## FUNCTIONAL MRI IN ASTHMATIC PATIENTS

### Studies of ventilation heterogeneity

MRI with hyperpolarized helium (HP He) provides a tool to visualize functional changes occurring in the distal small airways and lung parenchyma of asthmatic patients. A specific isotope of

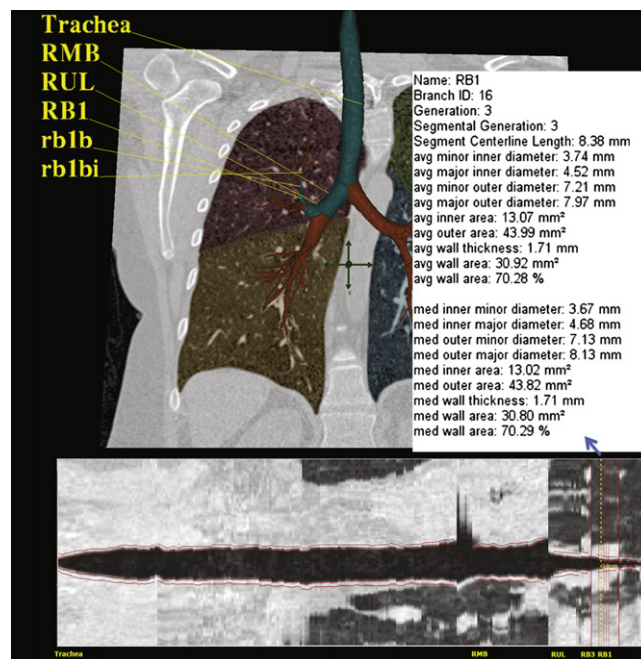


**FIG 3.** Three-dimensional and cross-sectional quantitative CT of the airway and lungs in asthmatic patients. Quantitative rendering of the airway tree in 3 dimensions with the RB1 segmental pathway highlighted with numeric quantitative airway dimensions (upper image) and in cross-section with airway boundaries outlined in red (lower image) is shown. RMB, Right main bronchus; RUL, right upper lobe.

helium ( $^3\text{He}$ ) can be brought into magnetic alignment outside of the magnetic resonance scanner (ie, "hyperpolarized") through interaction with a circularly polarized laser light by using either spin-exchange optical pumping<sup>81,82</sup> or metastability exchange.<sup>83</sup> The HP He gas can then be inhaled and allowed to physically distribute throughout the available airspace of the lungs, providing high-contrast images on MRI despite the low physical density of the gas. Regions of slow or obstructed ventilation will appear as signal voids, which are referred to as "ventilation defects."

The method is safe, requires no ionizing radiation dose, and can be repeatedly inhaled, facilitating longitudinal,<sup>84,85</sup> interventional,<sup>86</sup> and pediatric<sup>87</sup> examination. The polarized signal decays away to thermal equilibrium in 1 to 2 minutes<sup>88</sup> and washes out of the lung airspaces in a similar time frame.<sup>89</sup> There is now extensive experience with the use of HP He MRI in asthmatic patients, and only mild adverse events have been reported in less than 10% of subjects.<sup>90-92</sup> The primary safety concern is that the anoxic He-N<sub>2</sub> gas mixture displaces the air in the lungs, but even for extended breath holds of 10 to 20 seconds, the hemoglobin saturation rarely decreases to less than 90% and recovers to normal within a few seconds.<sup>92</sup> One important limitation of MRI is the paucity of anatomic detail available through conventional proton MRI, leading to a general inability to obtain anatomic correlates to the HP He image (Fig 4, A). Consequently, it is generally difficult to ascribe cause and effect regarding the functional information provided by HP He. Recent work has registered quantitative CT with HP He MRI images of ventilation to demonstrate that airway wall thickness (WT) increases proximal to ventilation defects on HP He MRI to resolve this limitation and provide structure-function assessment.<sup>93</sup>

Although CT, MRI, and PET have documented surprisingly large subsegmental and even segmental ventilation defects in patients with asthma,<sup>94-96</sup> HP He MRI is distinguished by its ability to provide images of ventilation with whole-lung coverage at relatively high spatial resolution, depicting the regional distribution of focal defects in asthmatic patients.<sup>97</sup> These defects are identified as regions with no or reduced signal because the airspaces distal to the obstruction do not fill relative to the surrounding areas (Fig 4, C). The resulting pattern of spatial heterogeneity is now recognized as a characteristic of asthma.<sup>98</sup> Nonetheless, the high level of heterogeneity revealed by HP He MRI in asthmatic patients is surprising, especially given that defects are observed even in asymptomatic patients and appear to involve the larger central airways (Fig 4, H). Thus He MRI provides support to the concept that asthma is heterogeneous in its manifestation within a given patient<sup>73,97,99</sup> and within the population of patients with severe asthma.<sup>100-102</sup>

Imaging of lung function with HP He MRI has allowed the discovery of local areas of airway obstruction in asthmatic patients that are heterogeneous and occur more frequently in those with severe asthma.<sup>94,103</sup> Moreover, ventilation defects in healthy subjects (Fig 4, D) are relatively common, although these defects are typically small (<3 cm) and confined to the peripheral regions of the lungs.<sup>103,104</sup> Consequently, there is substantial overlap between healthy volunteers and asthmatic patients with respect to the number of ventilation defects, although, on average, the lungs of asthmatic patients have more numerous and larger defects that become more pronounced as disease severity increases.<sup>103</sup> Although it remains possible that some of these healthy subjects have early-onset disease,<sup>105</sup> further study of the reproducibility and sensitivity of ventilation defect measures is required before this can be claimed definitively.

Interestingly, more than half of the defects in asthmatic patients have been found to persist over several days to more than a year.<sup>84</sup> A more systematic study found that 75% of defects were reproducible day to day and that a similar number did not change in size,<sup>85</sup> challenging the common perception of asthma as a dynamic disease with highly reversible sites of airway obstruction. In these studies the persistence of ventilation defects was found to be independent of asthma severity and medication use, suggesting that these defects are refractory to therapy. These results suggest that a more progressive structural remodeling of the large and small airways at specific regions of the lungs might reflect local airway injury and progressive loss of lung function.

Control of lung volume at breath hold in HP He MRI is important for standardizing and quantifying ventilation defect measures. In recent studies the volume of He-N<sub>2</sub> mixture was adjusted to the patient's TLC to normalize the inflation volume across patients.<sup>94,106</sup> Respiratory maneuvers, such as forced expirations<sup>107</sup> and deep inspirations,<sup>86</sup> can be performed in conjunction with interventions, such as exercise challenge, to further investigate the effects of inflation volume (see this month's cover image [September 2011]).

Respiratory maneuvers during fast MRI can depict the kinetics of airway obstruction. Dynamic images of inspiration and forced exhalation (Fig 5) have verified spatial heterogeneity and demonstrated temporal heterogeneity in the uptake and washout periods of HP He in asthmatic patients.<sup>107,108</sup> Regions of gas trapping in asthmatic patients were shown to reflect independent measures of lung function with plethysmography (ie, RV) and spirometry (ie, FEV<sub>1</sub> and FEV<sub>1</sub>/forced vital capacity ratio) and matched well

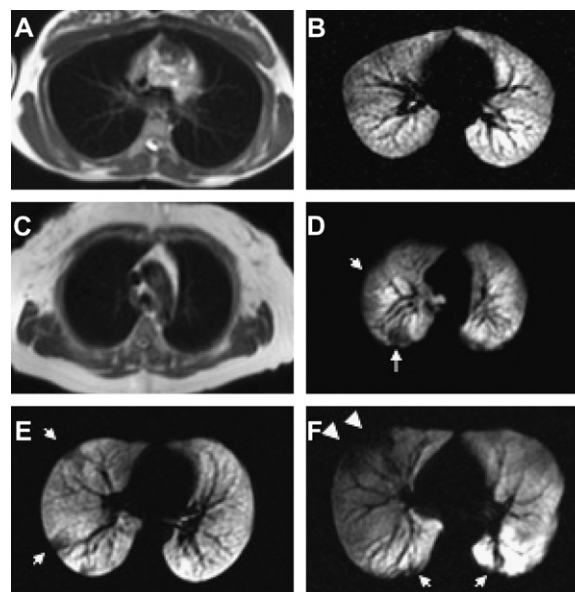


**FIG 4.** Magnetic resonance of lungs in healthy subjects and asthmatic patients. Examples of conventional proton magnetic resonance images paired with corresponding slices from HP He MRI in a healthy subject without ventilation defects (A and B) and a healthy subject with ventilation defects (C and D, arrows) are shown. Results of HP He MRI in a patient with mild-to-moderate persistent asthma (E) and severe asthma (F) are shown. Note the greater central extent of the defects more typical of severe asthma (Fig 4, F, arrowheads).

with low-density regions on MDCT images acquired at FRC. Emerging dynamic imaging techniques show promise for the depiction of respiratory dynamics in asthmatic patients with whole lung coverage and robustness, even in circumstances of loss of a patient's breath hold.

### Quantification of ventilation images

The development of objective quantitative measures of these ventilation defects is critical to the advance of HP He MRI. The most common metric used previously was the mean number of ventilation defects per slice. Although this and similar scores are simple and well suited to consensus evaluation in blinded studies,<sup>103</sup> they typically condense the defect pattern into a single whole-lung metric that does not effectively capture regional information. Quantitative regional measurements normalize defect volume to total lung volume and lung lobe accounting for both defect size and distribution<sup>94,109</sup> and, in cases of repeated studies, normalize to baseline signal values to calculate fractional ventilated volume.<sup>86</sup> Alternatively, a spatial coefficient of variation can be used to measure signal heterogeneity regionally.<sup>86</sup> This has been used effectively to show persistence of heterogeneity after deep inspiration in asthmatic patients compared with healthy volunteers after methacholine challenge.<sup>86</sup>

There are several emerging techniques using diffusion-weighted HP He MRI that are sensitive to physical diffusion of the gas within the airway and alveolar structures. The apparent diffusion coefficient (ADC) provides a quantitative measure of the size of the airspaces and has been shown to be highly reproducible<sup>110,111</sup> in healthy volunteers and patients with chronic obstructive pulmonary disease<sup>112-115</sup> and sensitive to

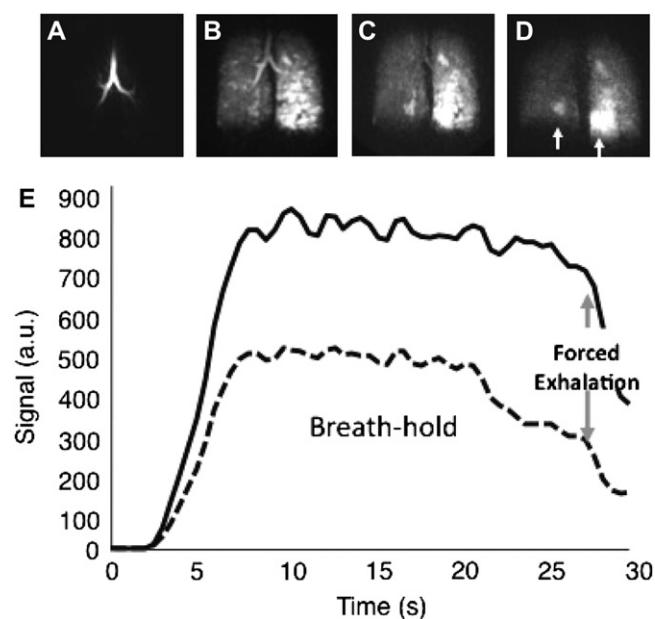


**FIG 5.** Functional magnetic resonance in asthmatic patients. Three-dimensional dynamic HP He MRI showing gas wash-in (**A**), breath hold (**B**), and forced expiration (**C** and **D**) at a 0.5-second frame rate for a patient with moderate persistent asthma demonstrating heterogeneous gas distribution (Fig 5, **B**) with gas trapping in the lower right and, most prominently, in the lower left lung (Fig 5, **C** and **D**, arrows) is shown. **E**, Kinetics of wash-in and washout derived from regions of interest in the right upper lobe (dotted) and left upper lobe (solid) can be used to quantify regional spirometry.

early disease and changes caused by aging.<sup>114,115</sup> Although the ADC measure applied to alveolar structures has thus far shown limited application to the study of asthma, recent work investigating larger-scale structures has measured significant differences between asthmatic patients and healthy subjects,<sup>116</sup> suggesting large airway or collateral ventilation abnormalities.<sup>117</sup> Specific models of lung structure<sup>118</sup> might also help to quantify the dimensions of the lung microstructures in asthmatic patients by using HP He MRI, allowing changes in airway structure to be tracked longitudinally for evaluating the response to therapy.

Xenon-129 (<sup>129</sup>Xe) is another noble gas that can be polarized by using the spin-exchange optical pumping method.<sup>119</sup> The fractional solubility of <sup>129</sup>Xe in the blood stream (approximately 17%)<sup>120</sup> has implications for measuring parameters related to the alveolar ventilation/perfusion ratio, which might be important in asthmatic patients to provide an assessment of an individual's ability to adapt to persistent obstruction, exacerbation, or both because of heterogeneity in ventilation. The application of HP <sup>129</sup>Xe MRI has lagged behind HP He methods largely because <sup>129</sup>Xe is more challenging to polarize<sup>82</sup> and has a lower gyromagnetic ratio than <sup>3</sup>He (11.8 vs 32.4 MHz/T) and because protocols for its application are not as fully developed. The recent shortage of <sup>3</sup>He has led to more serious development of <sup>129</sup>Xe MRI, and with technical advances in parallel MRI and improvements in <sup>129</sup>Xe polarization,<sup>121</sup> several encouraging preclinical studies<sup>122-124</sup> and promising pilot studies in human subjects<sup>125,126</sup> have been reported.

As with many functional imaging methods, there remain significant challenges to translating these methods to the clinic. However, the unique ability to visualize local airway obstruction

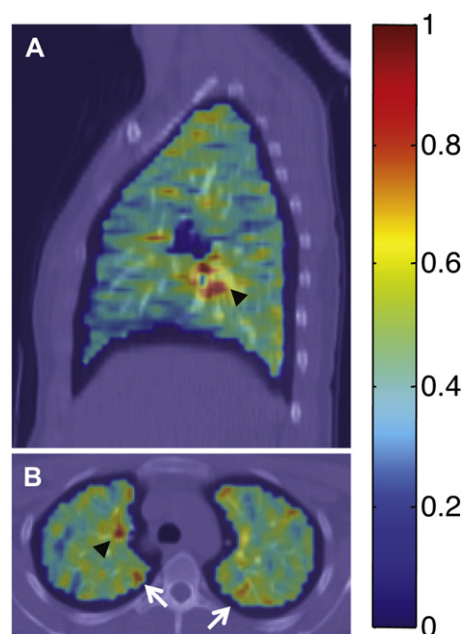


**FIG 6.** PET imaging of the lungs. FDG-PET/CT images depicting standardized uptake value parametric maps overlaid on CT images for a subject with mild persistent asthma during a respiratory tract infection are shown. Areas of uptake on both sagittal (**A**) and axial (**B**) slices indicate mediastinal lymph node inflammation (black arrowheads) and selected peripheral areas of localized airway inflammation (Fig 6, **B**, white arrows) are shown.

and explore the mechanisms and progression of airway obstruction longitudinally is an important strength of hyperpolarized gas MRI, especially as it pertains to the study of children with asthma without requiring ionizing radiation in this sensitive population. There is an increasing recognition that different phenotypes of asthma exist<sup>101</sup> and that these clusters of phenotypes might have differential responses to therapy. Moreover, as therapies become more diverse and patient specific, functional imaging will likely be one of the key ways to verify the response and efficacy to new therapies, and this will require a safe, longitudinal, and non-invasive method to assess the airway response before and after treatment. However, current functional imaging techniques need to become more quantitative, sensitive, and accessible to justify their current cost and complexity.

## MOLECULAR IMAGING IN ASTHMA

Molecular imaging has been broadly defined as the use of imaging methods that “directly or indirectly monitor and record the spatiotemporal distribution of molecular or cellular processes for biochemical, biologic, diagnostic, or therapeutic applications.”<sup>127</sup> Radiotracer imaging with nuclear medicine techniques is the modality that has been most frequently applied, although magnetic resonance spectroscopy and imaging, ultrasonography, and optical imaging also have served as molecular imaging modalities. Molecular imaging techniques are still largely under development, and their application to the study of asthma has been very limited. Those that have been identified as having potential applications in asthma include PET and SPECT.<sup>128,129</sup> Combination PET-CT systems allow improved correlation of PET signal abnormalities to specific anatomic structures (Fig 6).

Molecular imaging with PET requires coupling a positron-emitting radioisotope with a short half-life, such as  $^{18}\text{F}$ ,  $^{11}\text{C}$ , or  $^{15}\text{O}$ , to a molecule that functions within a known metabolic pathway. The most commonly used molecule in PET imaging is  $^{18}\text{F}$ -fluorodeoxyglucose ( $^{18}\text{F}$ -FDG), a radiolabeled glucose analog. When injected intravenously, FDG is transported into metabolically active cells and phosphorylated by the enzyme hexokinase in the same manner as glucose. However, the FDG-6-phosphate is not metabolized further and becomes trapped intracellularly, resulting in an increase in signal from the metabolically active cells.

FDG-PET is most commonly used in oncologic imaging because of its ability to depict the increased glucose metabolism present in most malignant neoplasms. However, FDG-PET also has shown promise as an imaging biomarker of lung inflammation. The accumulated evidence suggests that primed and activated neutrophils are the primary (although perhaps not the only) source of increased FDG signal in the lung.<sup>130</sup> In animal models increased FDG uptake has been demonstrated in acute lung injury<sup>131,132</sup> and after inhalation of cigarette smoke.<sup>133</sup> In human subjects increases in FDG uptake have been found in several conditions characterized by inflammation, such as respiratory tract infections (Fig 6), including pneumonia,<sup>134</sup> cystic fibrosis,<sup>135</sup> sarcoidosis,<sup>136,137</sup> and chronic obstructive pulmonary disease.<sup>138</sup>

The ability to quantify a component of the inflammatory response with FDG-PET suggests that it might also be useful for learning more about the pathogenesis of asthma, phenotypic differences, and responses to anti-inflammatory therapies. One study<sup>139</sup> demonstrated increased regional FDG signal in 5 patients with atopic asthma after bronchoscopic allergen challenge, although there was no increase in signal with inhaled allergen challenge. Another study<sup>138</sup> showed no difference in FDG uptake among 6 subjects with asthma and five healthy control subjects. However, this latter study also performed PET imaging with an agent that binds to macrophage receptors,  $^{11}\text{C}$ -labeled PK11195, and found that uptake was markedly higher in 3 of 5 asthmatic patients compared with that seen in healthy control subjects.<sup>134,140-142</sup>

Nuclear medicine imaging methods, such as SPECT with leukocytes labeled with  $^{111}\text{In}$  or  $^{99\text{m}}\text{Tc}$ , might identify the presence of an inflammatory response.<sup>130,143-161</sup> The radiopharmaceutical  $^{99\text{m}}\text{Tc}$ -exemetazime (technetium  $^{99\text{m}}$ -hexamethylpropylene amine oxime [ $^{99\text{m}}\text{Tc}$ -HMPAO]) has been recognized as a potential imaging agent for quantification of the lung reduction-oxidation potential. In its lipophilic form  $^{99\text{m}}\text{Tc}$ -HMPAO diffuses into the cell, where it is reduced to its hydrophilic form in the presence of GSH and remains trapped.<sup>162</sup>  $^{99\text{m}}\text{Tc}$ -HMPAO uptake is negligible in healthy lungs but is significantly increased in lungs with oxidative stress and inflammation. For example, active smokers have increased uptake in the lung that is proportional to the amount of cigarettes smoked.<sup>163,164</sup> Furthermore, irradiation injury to the lung, which is directly related to reactive oxygen species and reactive nitrogen species levels, is associated with markedly increased uptake of  $^{99\text{m}}\text{Tc}$ -HMPAO by the lung.<sup>163,164</sup> Although the spatial resolution of clinical SPECT is relatively poor (approximately 15 mm) in comparison with that of other modalities, such as PET, it appears sufficient for quantitative assessment of regional airway redox and inflammation. Taken together, HMPAO-SPECT-CT might be an innovative imaging modality for the airway inflammation of asthma, as it is in cigarette smoke-related lung disease.

## ALTERNATIVE IMAGING STRATEGIES IN ASTHMATIC PATIENTS

Nonradiographic imaging techniques might also be useful for imaging remodeling in asthma. Optical coherence tomography (OCT) is a new imaging method that combines near-infrared light with bronchoscopy to produce a 2-dimensional image of the airway wall. By using a fiberoptic catheter, OCT directs half of the infrared light to the tissue surface and the other half to a moving mirror; the reflected light is captured by a detector.<sup>79</sup> The technique allows the sampling of different layers of tissue with a spatial resolution of 3 to 16  $\mu\text{m}$  and depth penetration of 2 mm. Coxson et al<sup>80</sup> found that there was a correlation between CT and OCT measurements of lumen and wall area (WA) in former and current smokers. Furthermore, they found a strong correlation between FEV<sub>1</sub> percent predicted and OCT measurements of WA at the fifth-generation airways but not proximally. This new imaging technique can potentially provide both a microscopic view of airway WT and the subepithelial matrix and alveolar attachments. However, standards for this technique have not yet been formulated; it is subject to respiratory cycle movements and has not been studied in patients with other diseases, including asthma.

Two reports<sup>165,166</sup> describe the promising application of endobronchial ultrasonography (EBUS) in assessment of airway WT. EBUS is performed through fiberoptic bronchoscopy with an ultrasound probe within a balloon sheath inserted through the working channel. Airways of internal diameter as small as approximately 4 mm can be accessed by means of EBUS. EBUS enables visualization of multiple layers of the airway wall, including the mucosa, submucosa, smooth muscle, and outer layers of cartilage. Studies with EBUS imaging in asthmatic patients revealed that the inner mucosa and secondary layer of the submucosa and smooth muscle of the airway wall were thicker than in healthy control subjects.<sup>165,166</sup> Moreover, the total airway WT determined by using EBUS in this study was in good agreement with measures made by means of high-resolution CT, and the procedure of EBUS was well tolerated. Advantages of EBUS include the ability to determine regional airway wall remodeling serially for repeated measurements without radiation exposure.

## APPLICATION OF CT IMAGING IN ASTHMATIC PATIENTS

The vast majority of the studies of imaging in asthmatic patients have used CT. CT is the only widely available imaging modality and has been studied in a wide range of asthmatic patients and evaluated in the context of phenotype, traditional physiology, pathology, and treatment responses. Two general CT approaches have been used to evaluate and compare structural remodeling changes in the lung that occur in asthmatic patients with clinical and pathophysiologic parameters. These 2 approaches have focused on lung density measures, primarily as a measure of emphysema, air trapping, or both, and airway wall measures.

### Lung density measures

Different parameters have been used for density measures depending on whether the focus is emphysema or air trapping in patients with severe asthma. In earlier asthma studies the scans are generally done at TLC by using a threshold density of  $-910$  HU or less to define hyperinflated portions of the lung.<sup>167,168</sup> By using

this approach, decreased lung density at TLC was associated with greater airflow limitation. A dynamic component to these changes in lung density in asthmatic patients has also been suggested in studies stimulating bronchoconstriction with methacholine or exposure to cat dander. After 6 hours of exposure to cat dander, there was a significant increase in lung attenuation consistent with air trapping. This was accompanied by a significant decrease in forced expiratory fraction at 25% to 75% flow, which is consistent with small airway closure.<sup>169</sup> Similarly, decreased density was shown to be greater in a patient with an exacerbation of asthma, which partially reversed with treatment of the exacerbation.

In more recent studies, lung density has been evaluated at partial and full expiration (FRC and RV). Unlike the scans at TLC, these scans might better reflect the degree of air trapping, with one study suggesting that the ratio of lung attenuation area of less than  $-960$  HU at full inspiration compared with RV was negatively associated with forced expiratory fraction at 25% to 75% flow and positively correlated with RV/TLC, all of which is consistent with air trapping and small-airway disease.<sup>170</sup>

In studies from the Severe Asthma Research Program (SARP), the degree of air trapping as measured by the percentage of lung at less than  $-850$  HU at partial expiration (FRC) was shown to be associated with increasing severity of disease, specifically an increased likelihood of very severe exacerbations (Fig 7).<sup>52</sup> That study went on to address risk factors for this “air-trapping” phenotype. In the 117 subjects evaluated, atopy, increased neutrophilic inflammation, duration of disease, and history of pneumonia were all found to be independent predictors of air trapping by means of CT. Whether specific neutrophil-related processes in these patients with severe asthma, such as matrix modification by elastases or proteinases, is leading to this air trapping will require further study. Although prospective studies are necessary, this study suggests that quantitative CT imaging might be useful in identifying asthmatic patients with very high-risk disease.

All CT density studies to date have focused on global air trapping or hyperinflation. However, recent software improvements can now measure regional (lobar) differences in lung density to more precisely define the anatomic changes in relation to disease (Fig 2). Whether these general or regional differences in lung lucency portend different clinical scenarios, pathobiology and treatment options remain to be determined.

### Airway wall thickening

In addition to lung density data, MDCT imaging can precisely measure airway WT. Although quantitative CT imaging allows precise measurement of airway WT throughout the tracheobronchial tree, for ease of analysis, many early studies focused on a single airway to the right upper lobe (eg, RB1). However, measurements from this single airway likely do not represent the full spectrum of airway changes given the substantial segmental variability noted in patients with severe asthma.<sup>171,172</sup>

Airway wall measurements have included WA percentage, WA/body surface area, and thickness/diameter ratios. Studies have long reported increased wall thickening in relationship to more severe disease and even near-fatal asthma.<sup>171,173,174</sup> As part of SARP, the average WT and WA percentages were increased in subjects with severe asthma, although no specific segmental airway could be identified as most involved, and in fact, there was considerable heterogeneity among the airways.<sup>172</sup> However, in contrast to some studies, this general increase in airway WT

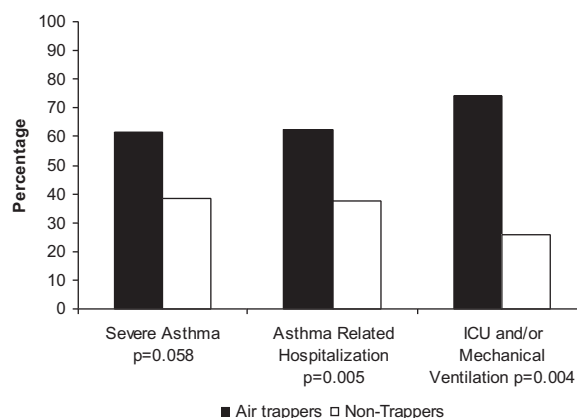


**FIG 7.** Air trapping and severe exacerbations. The presence of air trapping is associated with severe asthma and severe exacerbations of asthma. ICU, Intensive care unit. Reproduced with permission from Busacker et al.<sup>52</sup>

and WA percentages was found to be correlated with lung function, including FEV<sub>1</sub> and bronchodilator response. Interestingly, at least 1 study suggests that although increased wall thickening might be associated with more “severe” asthma, as measured by FEV<sub>1</sub>, airway wall thickening might have protective effects on bronchial hyperreactivity.<sup>175</sup> Although the clinical implications of this finding remain unclear, this study highlights the many possible studies that can be done with CT imaging to better understand structure-function relationships.

### Relationship to inflammation/remodeling

Several studies have attempted to link cellular and proteolytic properties to airway WT, as measured by means of CT. One of the first studies to address the relationship of pathologic changes to CT structural changes suggested that subepithelial basement membrane thickening measured histologically was highly correlated with both airway WA and WT percentages in a group of asthmatic and control subjects.<sup>176</sup> Similarly, the recent SARP study also correlated pathologic structural changes with CT airway measurements, suggesting moderate correlations between epithelial layer thickness and WA and WT percentages.<sup>172</sup> Thus quantitative CT scans might be a surrogate noninvasive measure of remodeling of the airways.

Additional studies relating inflammatory changes found in sputum, bronchoalveolar lavage fluid, or airway tissue to CT structure are needed. Two small studies have been published, with the first showing that the lower the ratio of matrix metalloproteinase 9/tissue inhibitor of metalloproteinase 1 in sputum, the greater the airway WT as measured by WA percentage.<sup>177</sup> A second study reported correlations between airway WT (as measured by the slope of WA/lumen area change by generation across all visible segments) and subepithelial basement membrane thickening and number of inflammatory cells infiltrating the bronchial mucosa.<sup>34</sup> However, this is likely only the beginning of potential links of imaging in asthmatic patients to the underlying pathobiology of asthma.

### Evaluating therapies

Use of quantitative imaging is particularly desirable for long-term studies and treatment trials of asthmatic patients in which repeated bronchoscopies might not be desirable. In fact, this

might be one of the most important clinical research applications of CT imaging. CT imaging has been used to evaluate the effect of inhaled corticosteroids, leukotriene receptor antagonists, and even new biologic agents, such as antibodies to IL-5, looking at both lung density and airway wall measurements.

Lung density measures (looking at change in lung attenuation from baseline to after treatment) have been reported to show the rather substantial effect of inhaled corticosteroids to decrease lung attenuation and improve air trapping over a 3-month period in patients with mild asthma. However, there were no differences observed between a fine-particle aerosol versus a more traditional particle size.<sup>178</sup> Of note, physiologic measures were not as able to pick up changes after treatment as CT changes. Another study that addressed the effect of a systemic medication on lung attenuation noted similar improvements in air trapping.<sup>179</sup> Although there were only modest improvements in FEV<sub>1</sub> percent predicted observed to go along with this increase, significant decreases in lung attenuation were seen after treatment with montelukast.

WA percentage has also been reported to decrease in response to inhaled corticosteroid therapy. A small but significant decrease in WA percentage, as measured by means of quantitative CT, was reported after treatment with a moderate dose of inhaled corticosteroid (beclomethasone, 800 µg/d for 12 weeks).<sup>180</sup> This decrease was correlated with the decrease in serum eosinophilic cationic protein levels, suggesting that the CT changes were related to the effect of corticosteroids on eosinophilic inflammation. An effect through eosinophils was supported by a recent study of patients with severe eosinophilic asthma treated with mepolizumab, an IL-5 mAb, which also demonstrated a significant reduction in RB1 WA percentage/body surface area in comparison with placebo.<sup>181</sup> Furthermore, a study of bronchial thermoplasty, a bronchoscopic procedure in which controlled thermal energy is applied to the airway wall to decrease smooth muscle, in patients with severe persistent asthma performed qualitative CT in a subset of participants: 100 were treated with thermoplasty, and 50 received sham bronchoscopy. Qualitative analysis of these CT scans demonstrated no evidence of airway or parenchymal injury related to bronchial thermoplasty and an increase in bronchial wall thickening in those receiving sham bronchoscopy at 1 year.<sup>182</sup> These studies demonstrate the potential use of quantitative imaging in asthmatic patients as a surrogate end point for airway remodeling in response to promising therapies or interventions.

### Need for standardization

Current lung-imaging modalities in practice lack methods of standardization with use of various scanners, software versions, and image-acquisition protocols to ensure reproducibility across sites. It is unclear whether regular water and air calibration can prevent these inconsistencies, especially with longitudinal examinations in which drift over time might mimic disease progression.<sup>183</sup> Networks (including the SARP) have started to use common CT phantoms to ensure reliability across centers and time to overcome these limitations in clinical trials. Care must be taken to ensure that the phantom contains differing objects of varying densities and consistency to capture the breadth of potential imaging modalities. However, standardization of other quantitative imaging measures (eg, ADC and ventilation defects) by using modalities such as MRI or PET is needed.

In addition to use of phantoms, use of specific imaging protocols is needed to optimize standardization in defining

disease status or making lung density or airway measurements. For example, in SARP subjects are coached to TLC in a standard fashion across sites. Alternatively, confirmation of lung volumes can be confirmed by using spirometric measurements at the time of image acquisition. A recent study suggests that sensitivity with repeated CT is improved when volumetric correction is applied by using individual patient data.<sup>184</sup> Lastly, establishing normal airway and lung density measurements in healthy populations is needed to help researchers better define deviations from the normal expected variation.

### Radiation exposure

The expansion of CT use in medicine has led to concern about the potential risk of excess cancers that is equally important in the consideration of research imaging. Chest CT examinations (3-6 mSv) deliver 60 to 120 times the radiation dose of a normal posterior anterior chest radiograph (0.05 mSv).<sup>185</sup> Furthermore, Smith-Bindman et al<sup>186</sup> recently demonstrated that because of lack of standardization in clinical practice, radiation dose varies widely (mean 13-fold variation) within and across institutions for the same type of study. The radiation dose associated with clinical CT examinations performed in 2007 in the United States accounted for a projected 29,000 excess cancers, with chest examinations accounting for a quarter of these.<sup>187</sup> In addition, this increased risk is greatest for women and younger patients.<sup>187,188</sup> Therefore CT chest examinations should be programmed with techniques that conform to the as-low-as-reasonably-achievable principal yet provide adequate image quality. Recent improvements in reconstruction algorithms, x-ray tube current modulation techniques, and use of breast and thyroid shields have helped minimize the radiation dose, especially to radiosensitive areas.<sup>185</sup>

With the consideration of risks associated with research CT imaging in asthmatic patients, care should be taken to minimize the dose consistent with the as-low-as-reasonably-achievable principal and to adequately inform adult participants of the risk associated with the research examination. Given the concern of increased radiation sensitivity in children, research CT in children with asthma should be avoided unless there is adequate justification of substantial benefit. One should balance the value of longitudinal CT examinations with the risk of increased radiation exposure over time. Furthermore, recent methods to quantify radiation dose exposure, such as the dose-length product, should be used so that serial radiologic examinations can calculate the cumulative radiation dose exposure over the course of the study.<sup>185</sup> Techniques to minimize this risk, such as low-dose CT scanning at 1 lung volume and use of dose-reduction algorithms, should be used.

### CONCLUSIONS

Imaging of the lungs in asthmatic patients by using standardized protocols can provide useful data leading to an improved understanding of the pathophysiology of asthma. These newer imaging modalities in asthmatic patients will provide us with new phenotypes of asthma as we begin to understand the structural and functional differences present in asthmatic patients, especially those with severe disease. As we develop better methods of standardization for quantitative CT and hyperpolarized gas MRI, we might be able to study earlier stages of disease and use these

measurements as end points for clinical trials. Recent studies<sup>180-182</sup> suggest that these imaging end points might be useful as targets for intervention. However, additional studies are needed to evaluate these methods in well-characterized cohorts over time.

## REFERENCES

- Benayoun L, Druilhe A, Dombret M-C, Aubier M, Pretolani M. Airway structural alterations selectively associated with severe asthma. *Am J Respir Crit Care Med* 2003;167:1360-8.
- Boulet L, Belanger M, Carrier G. Airway responsiveness and bronchial-wall thickness in asthma with or without fixed airflow obstruction. *Am J Respir Crit Care Med* 1995;152:865-71.
- Paganin F, Seneterre E, Chanez P, Dures J, Bruel J, Michel F, et al. Computed tomography of the lungs in asthma: influence of disease severity and etiology. *Am J Respir Crit Care Med* 1996;153:110-4.
- Pontana F, Faivre J, Remy-Jardin M, Flohr T, Schmidt B, Tacelli N, et al. Lung perfusion with dual-energy multidetector-row CT (MDCT): feasibility for the evaluation of acute pulmonary embolism in 117 consecutive patients. *J Thorac Imaging* 2008;25:100-11.
- Hoffman E, Chon D. Computed tomography studies of lung ventilation and perfusion. *Proc Am Thorac Soc* 2005;2:492-8, 506.
- Ritman E, Robb R, Harris L. Imaging physiological functions: experience with the DSR. Philadelphia: Praeger; 1985.
- Hoffman E, Ritman E. Effect of body orientation on regional lung expansion in dog and sloth. *J Appl Physiol* 1983;59:481-91.
- Boyd DP, Lipton MJ. Cardiac computed tomography. *Proc IEEE* 1983;71:298-307.
- Kalender W, Fichete H, Bautz W, Skalej M. Semiautomatic evaluation procedures for quantitative CT of the lung. *J Comput Assist Tomogr* 1991;15:248-55.
- Saito T, Misaki M, Shirato K, Takishima T. Three-dimensional quantitative coronary angiography. *IEEE Trans Biomed Eng* 1990;37:768-77.
- Saito Y. Multislice X-ray CT scanner. *Med Rev* 1998;98:1-8.
- Wang G, Lin T, Cheng P, Shinozaki D. A general cone-beam reconstruction algorithm. *IEEE Trans Med Imaging* 1993;12:486-96.
- Christensen G, Carlson B, Chao K, Yen P, Grigsby P, Nguyen K, et al. Image-based dose planning of intracavitary brachytherapy: registration of serial imaging studies using deformable anatomic templates. *Int J Radiat Oncol Biol Phys* 2001;51:227-43.
- Ding K, Christensen G, Hoffman E, Reinhardt J. Registration-based regional lung mechanical analysis: retrospectively reconstructed dynamic imaging versus static breath-hold image acquisition. Presented at: SPIE Conference; 2009; Lake Buena Vista, Fla.
- Ding K, Cao K, Christensen G, Raghavan M, Hoffman E, Reinhardt J. Registration-based lung tissue mechanics assessment during tidal breathing. Presented at: First International Workshop on Pulmonary Image Analysis; 2008; New York, NY. p. 63-72.
- Sanders C, Nath P, Bailey W. Detection of emphysema with computed tomography correlation with pulmonary function tests and chest radiography. *Invest Radiol* 1988;23:262-6.
- Wollmer P, Albrechtsson U, Brauer K, Eriksson L, Jonson B, Tylen U. Measurement of pulmonary density by means of x-ray computerized tomography. *Chest* 1986;90:387-91.
- Vock P, Salzmann C. Comparison of computed tomographic lung density with haemodynamic data of the pulmonary circulation. *Clin Radiol* 1986;37:459-64.
- Amirav I, Kramer S, Grunstein M, Hoffman E. Assessment of methacholine-induced airway constriction by ultrafast high-resolution computed tomography. *J Appl Physiol* 1993;75:2239-50.
- Wood S, Zarhouni E, Hoford J, Hoffman E, Mitzner W. Measurement of three-dimensional lung tree structures by using computed tomography. *J Appl Physiol* 1995;79:1687-97.
- Brown R, Pearce D, Pyrgos G, Liu M, Toghias A, Permutt S. The structural basis of airways hyperresponsiveness in asthma. *J Appl Physiol* 2006;101:30-9.
- Jarad N, Wilkenson P, Pearson M, Rudd R. A new high resolution computed tomography scoring system for pulmonary fibrosis, pleural disease, and emphysema in patients with asbestos related disease. *Br J Ind Med* 1992;49:73-84.
- Hoffman E, Simon B, McLennan G. State of the Art. A structural and functional assessment of the lung via multidetector-row computed tomography: phenotyping chronic obstructive pulmonary disease. *Proc Am Thorac Soc* 2006;3:519-32.
- Brown R, Herold C, Hirshman CZ, EA, Mitzner W. In vivo measurements of airway reactivity using high-resolution computed tomography. *Am Rev Respir Dis* 1991;144:208-212.
- Zerhouni E, Herold C, Brown R, Wetzel R, Hirshman C, Robotham J, et al. High-resolution computed tomography-physiologic correlation. *J Thorac Imaging* 1993;8:265-72.
- Brown R, Herold C, Hirshman C, Zerhouni E, Mitzner W. Individual airway constrictor response heterogeneity to histamine assessed by high-resolution computed tomography. *J Appl Physiol* 1993;74:2615-20.
- de Jong P, Muller N, Pare P, Coxson H. Computed tomographic imaging of the airways: relationship to structure and function. *Eur Respir J* 2005;26:140-52.
- Nakano Y, Wong J, de Jong P, Buzatu L, Nagao T, Coxson H, et al. The prediction of small airway dimensions using computed tomography. *Am J Respir Crit Care Med* 2005;171:142-6.
- Wood S, Zarhouni E, Hoford J, Hoffman E, Mitzner W. Quantitative 3-D reconstruction of airway and pulmonary vascular trees using HRCT. Presented at: SPIE Proceedings Biomedical Image Processing and Biomedical Visualization; 1993; San Jose, Calif. p. 316-23.
- Tschrirren J, Hoffman E, McLennan G, Sonka M. Intrathoracic airway trees: segmentation and airway morphology analysis from low dose CT scans. *IEEE Trans Med Imaging* 2005;24:1529-39.
- Tschrirren J, Hoffman E, McLennan G, Sonka M. Segmentation and quantitative analysis of intrathoracic airway trees from computed tomography images. *Proc Am Thorac Soc* 2005;2:484-7, 503-4.
- Tschrirren J, McLennan G, Palagyi K, Hoffman E, Sonka M. Matching and anatomical labeling of human airway tree. *IEEE Trans Med Imaging* 2005;24:1540-7.
- Hoshino M, Matsuoka S, Handa H, Miyazawa T, Yagihashi K. Correlation between airflow limitation and airway dimensions assessed by multidetector CT in asthma. *Respir Med* 2010;104:794-800.
- Montaudon M, Lederlin M, Reich S, Begueret H, Tunon-de-Lara J, Marthan R, et al. Bronchial measurements in patients with asthma: comparison of quantitative thin-section CT findings with those in healthy subjects and correlation with pathologic findings. *Radiology* 2009;253:844-53.
- Shimizu K, Hasegawa M, Makita H, Nasuhara Y, Konno S, Nishimura M. Airflow limitation and airway dimensions assessed per bronchial generation in older asthmatics. *Respir Med* 2010;104:1809-16.
- Hoffman E, Sinak L, Robb R, Ritman E. Noninvasive quantitative imaging of shape and volume of lungs. *J Appl Physiol* 1983;54:1414-21.
- Wananuki Y, Suzuki S, Nishikawa M, Miyashita A, Okubo T. Correlation of quantitative CT with selective alveolobronchogram and pulmonary function tests in emphysema. *Chest* 1994;106:806-13.
- Kinsella M, Muller N, Abboud R, Morrison N, DyBuncio A. Quantitation of emphysema by computed tomography using a "density mask" program and correlation with pulmonary function tests. *Chest* 1990;97:315-21.
- Muller N, Staples C, Miller R, Abboud R. "Density mask." An objective method to quantitate emphysema using computed tomography. *Chest* 1988;94:782-7.
- Gould G, Redpath A, Ryan M, Warren P, Best J, Cameron E, et al. Parenchymal emphysema measured by CT lung density correlates with lung function in patients with bullous disease. *Eur Respir J* 1993;6:698-704.
- Stern E, Frank M, Schmutz J, Glenny R, Schmidt R, Goodwin J. Panlobular pulmonary emphysema caused by IV injection of methylphenidate (ritalin): findings on chest radiographs radiographs and CT scans. *Am J Radiol* 1994;162:555-60.
- Newman K, Lynch D, Newman L, Ellegood D, Newell J. Quantitative computed tomography detects air trapping due to asthma. *Chest* 1994;106:105-9.
- Millar A, Fromson B, Strickland B, Denison D. Computed tomography based estimates of regional gas and tissue volume of the lung in supine subjects with chronic airflow limitation or fibrosing alveolitis. *Thorax* 1986;41:932-9.
- Reinmuller R, Behr J, Kalender W. Standardized quantitative high resolution CT in lung diseases. *J Comput Assist Tomogr* 1991;15:742-9.
- Biernacki W, Gould G, Whyte K, Flenley D. Pulmonary hemodynamics, gas exchange, and the severity of emphysema as assessed by quantitative CT scan in chronic bronchitis and emphysema. *Am Rev Respir Dis* 1989;139:1509-15.
- Gould K. Coronary artery stenosis. New York: Elsevier; 1991.
- Gould G, MacNee W, McLean A, Warren P, Redpath A, Best J, et al. CT Measurements of Lung Density in Life can quantitate distal airspace enlargement—an essential defining feature of human emphysema. *Am Rev Respir Dis* 1988;137:380-92.
- Knudson R, Standen J, Kaltenborn W, Knudson D, Rehm K, Habib M, et al. Expiratory computed tomography for assessment of suspected pulmonary emphysema. *Chest* 1991;99:1357-66.
- Hartley P, Galvin J, Hunninghake G, Merchant J, Yagla S, Speakman S, et al. High-resolution CT-derived measures of lung density are valid indexes of interstitial lung disease. *J Appl Physiol* 1994;76:271-7.
- Goris M, Blankenberg F, Chan F, Robinson T. An automated approach to quantitative air trapping measurements in mild cystic fibrosis. *Chest* 2003;123:1655-63.

51. Grenier PA, Beigelman-Aubry CF, Fetita C, Preteux F, Brauner M, Lenoir S. New frontiers in CT imaging of airway disease. *Eur Radiol* 2002;12:1022-44.
52. Busacker A, Newell J, Keefe T, Hoffman E, Granroth J, Castro M, et al. A multivariate analysis of risk factors for the air-trapping asthmatic phenotype as measured by quantitative CT analysis. *Chest* 2009;135:48-56.
53. Ball W, Stewart P, Newsham L, Bates D. Regional pulmonary function studied with Xenon-133. *J Clin Invest* 1962;41:519-31.
54. Jones R, Overton T, Sproule B. Frequency dependence of ventilation distribution in normal and obstructed lungs. *J Appl Physiol* 1977;42:548-53.
55. Bunow B, Line B, Horton M, Weiss G. Regional ventilatory clearance by xenon scintigraphy: a critical evaluation of two estimation procedures. *J Nucl Med* 1979;20:703-10.
56. Hubmayr R, Walters B, Chevalier P, Rodarte J, Olson L. Topographical distribution of regional lung volume in anesthetized dogs. *J Appl Physiol* 1983;54:1048-56.
57. Berdine G, Lehr J, McKinley D, Drazen J. Nonuniformity of canine lung washout by high-frequency ventilation. *J Appl Physiol* 1986;61:1388-94.
58. Fredberg J, Keefe D, Glass G, Castile R, Frantz I. Alveolar pressure nonhomogeneity during small-amplitude high-frequency oscillation. *J Appl Physiol* 1984;57:788-800.
59. Hubmayr R, Hill M, Wilson T. Nonuniform expansion of constricted dog lungs. *J Appl Physiol* 1996;80:522-30.
60. Robertson H, Glenny R, Stanford D, McInnes L, Luchtel D, Covert D. High-resolution maps of regional ventilation utilizing inhaled fluorescent microspheres. *J Appl Physiol* 1997;82:943-53.
61. van der Mark T, Rookmaker A, Kiers A, Peset R, Vaalburg W, Paans A, et al. Nitrogen-13 and xenon-133 ventilation studies. *J Nucl Med* 1984;25:1175-82.
62. Venegas J, Yamada Y, Custer J, Hales C. Effects of respiratory variables on regional gas transport during high-frequency ventilation. *J Appl Physiol* 1988;64:2108-18.
63. Gur D, Drayer B, Borovetz H, Griffith B, Hardesty R, Wolfson S. Dynamic computed tomography of the lung: regional ventilation measurements. *J Comput Assist Tomogr* 1979;3:749-53.
64. Gur D, Shabason L, Borovetz H, Herbert D, Reece G, Kennedy W, et al. Regional pulmonary ventilation measurements by xenon enhanced dynamic computed tomography: an update. *J Comput Assist Tomogr* 1981;5:678-83.
65. Marcucci C, Nyhan D, Simon B. Distribution of pulmonary ventilation using Xe-enhanced computed tomography in prone and supine dogs. *J Appl Physiol* 2001;90:421-30.
66. Tajik J, Chon D, Won C, Tran B, Hoffman E. Subsecond multisection CT of regional pulmonary ventilation. *Acad Radiol* 2002;9:130-46.
67. Simon B, Marcucci C, Fung M, Lele S. Parameter estimation and confidence intervals for Xe-CT ventilation studies: a Monte Carlo approach. *J Appl Physiol* 1998;84:709-16.
68. Chon D, Beck K, Simon B, Shikata H, Saba O, Hoffman E. Effect of low-xenon and krypton supplementation on signal/noise of regional CT-based ventilation measurements. *J Appl Physiol* 2007;102:1535-44.
69. Chon D, Simon B, Beck K, Shikata H, Saba O, Won C, et al. Differences in regional wash-in and wash-out time constraints for xenon-CT ventilation studies. *Respir Physiol Neurobiol* 2005;148:65-83.
70. Boroto K, Remy-Jardin M, Flohr T, Faivre J, Pansini V, Tacelli N, et al. Thoracic applications of dual-source CT technology. *Eur J Radiol* 2008;68:375-84.
71. Park E, Goo J, Park S, Lee H, Lee C, Yoo C, et al. Chronic obstructive pulmonary disease: quantitative and visual ventilation pattern analysis at xenon ventilation CT performed by using a dual-energy technique. *Radiology* 2010;256:985-97.
72. Kang M, Park C, Lee C, Goo J, Lee H. Dual-energy CT: clinical applications in various pulmonary diseases. *Radiographics* 2010;30:685-98.
73. Chae E, Seo J, Lee J, Kim N, Goo H, Lee H, et al. Xenon ventilation imaging using dual-energy computed tomography in asthmatics: initial experience. *Invest Radiol* 2010;45:354-61.
74. Fuld M, Saba O, Krauss B, Van Bleek E, McClennan G, Hoffman E. Dual Energy Xe-MDCT for Automated Assessment of the Central Airway Tree: initial Experiences. Presented at: American Thoracic Society Annual Meeting; 2007; San Francisco, Calif.
75. Wolfkiel C, Rich S. Analysis of regional pulmonary enhancement in dogs by ultrafast computed tomography. *Invest Radiol* 1992;27:211-6.
76. Won C, Chon D, Tajik J, Tran B, Robinsowood G, Beck K, et al. CT-based assessment of regional pulmonary microvascular blood flow parameters. *J Appl Physiol* 2003;94:2483-93.
77. Chon D, Beck K, Larsen R, Shikata H, Hoffman E. Regional pulmonary blood flow in dogs by 4D-X-ray CT. *J Appl Physiol* 2006;101:1451-65.
78. Alford S, Van Bleek E, McLennan G, Hoffman E. Heterogeneity of pulmonary perfusion as a mechanistic image-based phenotype in emphysema susceptible smokers. *Proc Natl Acad Sci U S A* 2010;107:7485-90.
79. Coxson H, Mayo J, Lam S, Santyr G, Parraga G, Sin D. New and current clinical imaging techniques to study chronic obstructive pulmonary disease. *Am J Respir Crit Care Med* 2009;180:588-97.
80. Coxson H, Quiney B, Sin D, Xing L, McWilliams A, Mayo J, et al. Airway wall thickness assessed using computed tomography and optical coherence tomography. *Am J Respir Crit Care Med* 2008;177:1201-6.
81. Bouchiat M, Carver T, Varnum C. Nuclear polarization in He gas induced by optical pumping and dipolar exchange. *Phys Rev Lett* 1960;5:373-5.
82. Walker T, Happer W. Spin-exchange optical pumping of noble-gas nuclei. *Rev Modern Phys* 1997;69:629-42.
83. Gentile T, Jones G, Thompson A, Rizi R, Roberts D, Dimitrov I, et al. Demonstration of a compact compressor for application of metastability-exchange optical pumping of <sup>3</sup>He to human lung imaging. *Magn Reson Med* 2000;43:290-4.
84. de Lange E, Altes T, Patrie J, Parmer J, Brookeman J, Mugler J, et al. The variability of regional airflow obstruction within the lungs of patients with asthma: assessment with hyperpolarized helium-3 magnetic resonance imaging. *J Allergy Clin Immunol* 2007;119:1072-8.
85. de Lange E, Altes T, Patrie J, Battsiton J, Juersvich A, Mugler J 3rd, et al. Changes in regional airflow obstruction over time in the lungs of patients with asthma: evaluation with <sup>3</sup>He MR imaging. *Radiology* 2009;250:567-75.
86. Tzeng Y, Lutchen K, Albert M. The difference in ventilation heterogeneity between asthmatic and healthy subjects quantified using hyperpolarized <sup>3</sup>He MRI. *J Appl Physiol* 2009;106:813-22.
87. Altes T, de Lange E. Applications of hyperpolarized helium-3 gas magnetic resonance imaging in pediatric lung disease. *Top Magn Reson Imaging* 2003;14:231-6.
88. Kauczor H, Surkau R, Roberts T. MRI using hyperpolarized noble gasses. *Eur Radiol* 1998;8:820-7.
89. Jolliet P, Tassaux D. Helium-oxygen ventilation. *Respir Care Clin North Am* 2002;8:295-307.
90. Altes TA, Gersbach JC, Mata JF, Mugler JP, 3rd, Brookeman JR, De Lange EE. Evaluation of the safety of hyperpolarized helium-3 gas as an inhaled contrast agent for MRI [abstr]. In: Proceedings of the Fifteenth Meeting of the International Society for Magnetic Resonance in Medicine. Berkeley, Calif: International Society for Magnetic Resonance in Medicine, 2007; 1305.
91. Fain S, Korosec F, Holmes J, O'Halloran R, Sorkness R, Grist T. Functional lung imaging using hyperpolarized gas MRI. *J Magn Reson Imaging* 2007;25:910-23.
92. Lutey B, Lefrak S, Woods J, Tanoli T, Quirk J, Bashir A, et al. Hyperpolarized <sup>3</sup>He MR imaging: physiologic monitoring observations and safety considerations in 100 consecutive subjects. *Radiology* 2008;248:655-61.
93. Peterson E, Dattawadkar A, Samimi K, Jarjour N, Busse W, Fain S. Airway measures on MDCT in asthma at locations of ventilation defect identified by He-3 MRI. *Am J Respir Crit Care Med* 2010;181:A3958.
94. Fain S, Gonzalez-Fernandez G, Peterson E, Evans M, Sorkness R, Jarjour N, et al. Evaluation of structure-function relationships in asthma using multidetector CT and hyperpolarized He-3 MRI. *Acad Radiol* 2008;15:753-62.
95. Tgavelkos N, Tawhai M, Harris R, Musch G, Vidal-Melo M, Venegas J, et al. Identifying airways responsible for heterogeneous ventilation and mechanical dysfunction in asthma: an image functional modeling approach. *J Appl Physiol* 2005;99:2388-97.
96. Altes T, Powers P, Knight-Scott J, Rakes G, Platts-Mills T, Lange E, et al. Hyperpolarized <sup>3</sup>He MR lung ventilation imaging in asthmatics: preliminary findings. *J Magn Reson Imaging* 2001;13:378-84.
97. Samee S, Altes T, Powers P, de Lange E, Knight-Scott J, Rakes G, et al. Imaging the lungs in asthmatic patients by using hyperpolarized helium-3 magnetic resonance: assessment of response to methacholine and exercise challenge. *J Allergy Clin Immunol* 2003;111:1205-11.
98. Bousquet J, Jeffrey P, Busse W, Johnson M, Vignola A. Asthma. From bronchoconstriction to airways inflammation and remodeling. *Am J Respir Crit Care Med* 2000;161:1720-45.
99. Tgavalekos N, Musch G, Harris R, Vidal Melo M, Winkler T, Schroeder T, et al. Relationship between airway narrowing, patchy ventilation and lung mechanics in asthmatics. *Eur Respir J* 2007;29:1174-81.
100. Lemanske R Jr, Busse W. Asthma: clinical expression and molecular mechanisms. *J Allergy Clin Immunol* 2010;125(suppl):S95-102.
101. Moore W, Bleeker E, Curran-Everett D, Erzurum S, Ameredes B, Bacharier L, et al. Characterization of the severe asthma phenotype by the National Heart, Lung, and Blood Institute's Severe Asthma Research Program. *J Allergy Clin Immunol* 2007;119:405-13.
102. Moore W, Meyers D, Wenzel S, Teague W, Li H, Li X, et al. Identification of asthma phenotypes using cluster analysis in the Severe Asthma Research Program. *Am J Respir Crit Care Med* 2010;181:315-23.

103. de Lange E, Altes T, Patrie J, Gaare J, Knake J, Mugler J 3rd, et al. Evaluation of asthma with hyperpolarized helium-3 MRI: correlation with clinical severity and spirometry. *Chest* 2006;130:1055-62.
104. Lee E, Sun Y, Zurakowski D, Hatabu H, Khatwa U, Albert M. Hyperpolarized 3He MR imaging of the lung: normal range of ventilation defects and PFT correlation in young adults. *J Thorac Imaging* 2009;24:110-4.
105. van Beek E, Dahmen A, Stavngaard T, Gast K, Heussel C, Krummenauer F, et al. Hyperpolarized 3-He MRI vs HRCT in COPD and normal volunteers-PHIL trial. *Eur Respir J* 2009;34:1311-21.
106. Diaz S, Casselbrant I, Piitulainen E, Pettersson G, Magnusson P, Peterson B, et al. Hyperpolarized 3He apparent diffusion coefficient MRI of the lung: reproducibility and volume dependency in healthy volunteers and patients with emphysema. *J Magn Reson Imaging* 2008;27:763-70.
107. Holmes J, O'Halloran R, Brodsky E, Jung Y, Block W, Fain S. 3D hyperpolarized He-3 MRI of ventilation using a multi-echo projection acquisition. *Magn Reson Med* 2008;59:1062-71.
108. Holmes J, O'Halloran R, Peterson E, Brodsky E, Bley T, Francois C, et al. Three dimensional imaging of ventilation dynamics in asthmatics using multi-echo projection acquisition with constrained reconstruction. *Magn Reson Med* 2009;62:1543-56.
109. Woodhouse N, Wild J, Paley M, Fichele S, Said Z, Swift A, et al. Combined helium-3/proton magnetic resonance imaging measurement of ventilated lung volumes in smokers compared to never-smokers. *J Magn Reson Imaging* 2005;21:365-9.
110. Diaz S, Casselbrant I, Piitulainen E, Magnusson P, Peterson B, Pickering E, et al. Progression of emphysema in a 12-month hyperpolarized 3He-MRI study: lacunarity analysis provided a more sensitive measure than standard ADC analysis. *Acad Radiol* 2009;16:700-7.
111. Diaz S, Casselbrant I, Piitulainen E, Magnusson P, Peterson B, Wollmer P, et al. Validity of apparent diffusion coefficient hyperpolarized 3He-MRI using MSCT and pulmonary function tests as references. *Eur J Radiol* 2009;71:257-63.
112. Saam B, Yablonsky D, Kodibagkar V, Leawoods J, Gierada G, Cooper J, et al. MR imaging of diffusion of 3He gas in healthy and diseased lungs. *Magn Reson Med* 2000;44:174-9.
113. Salerno M, Lange E, Altes T, Truwit J, Brookeman J, Mugler J. Emphysema: hyperpolarized helium-3 diffusion MR imaging of the lungs compared with spirometric indexes—initial experience. *Radiology* 2002;222:252-60.
114. Fain S, Altes T, Panth S, Evans M, Walters B, Mugler J 3rd, et al. Detection of age-dependent changes in healthy adult lungs with diffusion-weighted 3He MRI. *Acad Radiol* 2005;12:1385-93.
115. Fain S, Panth S, Evans M, Wentland A, Holmes J, Korosec F, et al. Early emphysematous changes in asymptomatic smokers: detection with 3He MR imaging. *Radiology* 2006;239:875-83.
116. Wang C, Altes T, Mugler J III, Miller G, Ruppert K, Malta J, et al. Assessment of the lung microstructure in patients with asthmas using hyperpolarized 3He diffusion MRI at two time scales: comparison with healthy subjects and patients with COPD. *J Magn Reson Imaging* 2008;28:80-8.
117. Bartel S, Haywood S, Woods J, Chang Y, Menard C, Yablonsky D, et al. Role of collateral paths in long-range diffusion in lungs. *J Appl Physiol* 2008;104:1495-503.
118. Yablonskiy D, Sukstanskii A, Leawoods J, Gierada D, Bretthorst G, Lefrak S, et al. Quantitative in vivo assessment of lung microstructure at the alveolar level with hyperpolarized 3He diffusion MRI. *Proc Natl Acad Sci U S A* 2002;99:3111-6.
119. Lodi U, Harding S, Coghlan C, Guzzo M, Walker L. Autonomic regulation in asthmatics with gastroesophageal reflux. *Chest* 1997;111:65-70.
120. MacDonald A, Wann K. *Physiological aspects of anesthetics and inert gasses*. London: Academic Press; 1978.
121. Ruset I, Ketel S, Hersman W. Optical pumping system design for large production of hyperpolarized 129Xe. *Phys Rev Lett* 2006;96:053002.
122. Ruppert K, Mata J, Brookeman J, Hagspiel K, Mugler J. Exploring lung function with hyperpolarized Xe-129 nuclear magnetic resonance. *Magn Reson Med* 2004;51:676-87.
123. Mansson S, Wobler J, Driehuys BW, Wollmer P, Golman K. Characterization of diffusing capacity and perfusion of the rat lung in a lipopolysaccharide disease model using hyperpolarized 129Xe. *Magn Reson Med* 2003;50:1170-9.
124. Abdeen N, Cross A, Cron G, White S, Rand T, Miller D, et al. Measurement of xenon diffusing capacity in the rat lung by hyperpolarized 129Xe MRI and dynamic spectroscopy in a single breath-hold. *Magn Reson Med* 2006;56:255-64.
125. Mugler JP 3rd, Altes TA, Ruset IC, Dregely IM, Mata JF, Miller GW, et al. Simultaneous magnetic resonance imaging of ventilation distribution and gas uptake in the human lung using hyperpolarized xenon-129. *Proc Natl Acad Sci U S A* 2010;107:21707-12.
126. Dregely I, Rupert K, Altes T, Ruset I, Mugler J, Hersman W. Lung function imaging with hyperpolarized xenon MRI in asthmatics. *Am J Respir Crit Care Med* 2010;181:A1265.
127. Thakur M, Lentle B. Report of a summit on molecular imaging. *Am J Roentgenol* 2006;186:297-9.
128. Harris R, Schuster D. Visualizing lung function with positron emission tomography. *J Appl Physiol* 2007;102:448-58.
129. Dolovich M, Schuster D. Positron emission tomography and computed tomography versus positron emission tomography computed tomography: tools for imaging the lung. *Proc Am Thorac Soc* 2007;4:328-33.
130. Chen D, Schuster D. Imaging pulmonary inflammation with positron emission tomography: a biomarker for drug development. *Mol Pharmacol* 2006;3:488-95.
131. Chen D, Schuster D. Positron emission tomography with [18F]fluorodeoxyglucose to evaluate neutrophil kinetics during acute lung injury. *Am J Physiol Lung Cell Mol Physiol* 2004;286:L834-40.
132. Musch G, Venegas JG, Bellani G, Winkler T, Schroeder T, Peterson B, et al. Regional gas exchange and cellular metabolic activity in ventilator-induced lung injury. *Anesthesiology* 2007;106:723-35.
133. Schroeder T, Vidal Melo M, Musch G, Harris R, Winkler T, Venegas J. PET imaging of regional 18F-FDG uptake and lung function after cigarette smoke inhalation. *J Nucl Med* 2007;48:413-9.
134. Jones H, Sriskandan S, Peters A, Pride N, Krausz T, Boobis A, et al. Dissociation of neutrophil emigration and metabolic activity in lobar pneumonia and bronchiectasis. *Eur Respir J* 1997;10:795-803.
135. Chen D, Ferkol T, Mintun M, Pittman J, Rosenbluth D, Schuster D. Quantifying pulmonary inflammation in cystic fibrosis with positron emission tomography. *Am J Respir Crit Care Med* 2006;173:1363-9.
136. Brudin L, Valind S, Rhodes C, Pantin C, Sweatman M, Jones T, et al. Fluorine-18 deoxyglucose uptake in sarcoidosis measured with positron emission tomography. *Eur J Nucl Med* 1994;21:297-305.
137. Xiu Y, Yu J, Cheng E, Kumar R, Alavi A, Zhuang H. Sarcoidosis demonstrated by FDG PET imaging with negative findings on gallium scintigraphy. *Clin Nucl Med* 2005;30:193-5.
138. Jones H, Marino P, Shakur B, Morrell N. In vivo assessment of lung inflammatory cell activity in patients with COPD and asthma. *Eur Respir J* 2003;21:567-73.
139. Taylor I, Hill A, Hayes M, Rhodes C, O'Shaughnessy K, O'Connor B, et al. Imaging allergen-invoked airway inflammation in atopic asthma with [18F]-fluorodeoxyglucose and positron emission tomography. *Lancet* 1996;347:937-40.
140. Schroeder T, Vidal Melo M, Musch G, Harris R, Venegas J, Winkler T. Modeling pulmonary kinetics of 2-deoxy-2-[18F]fluoro-D-glucose during acute lung injury. *Acad Radiol* 2008;15:763-75.
141. Patlak CB, RG, Fenstermacher J. Graphical evaluation of blood-to-brain transfer constants from multiple-time uptake data. *J Cereb Blood Flow Metab* 1983;3:1-7.
142. Patlak C, Blasberg R. Graphical evaluation of blood-to-brain transfer constants from multiple-time uptake data. Generalizations. *J Cereb Blood Flow Metab* 1985;5:584-90.
143. Rennen H, Boerman O, Oyen W, Corstens F. Imaging, infection/inflammation in the new millennium. *Eur J Nucl Med* 2001;28:241-52.
144. Aulak K, Miyagi M, Yan L, West K, Massillon D, Crabb J, et al. Proteomic method identifies proteins nitrated in vivo during inflammatory challenge. *Proc Natl Acad Sci U S A* 2001;98:12056-61.
145. Bast A, Haenen GR, Doelman CJ. Oxidants and antioxidants: state of the art. *Am J Med* 1991;91:2S-13S.
146. Calhoun WJ, Reed HE, Moest DR, Stevens CA. Enhanced superoxide production by alveolar macrophages and air-space cells, airway inflammation, and alveolar macrophage density changes after segmental antigen bronchoprovocation in allergic subjects. *Am Rev Respir Dis* 1992;145:317-25.
147. Comhair S, Bhatena P, Dweik R, Kavuru M, Erzurum S. Rapid loss of superoxide dismutase activity during antigen-induced asthmatic response. *Lancet* 2000;355:624.
148. Comhair S, Bhatena P, Farver C, Thunnissen F, Erzurum S. Extracellular glutathione peroxidase induction in asthmatic lungs: evidence for redox regulation of expression in human airway epithelial cells. *FASEB J* 2001;15:70-8.
149. Comhair S, Xu W, Ghosh S, Thunnissen F, Almasan A, Calhoun W, et al. Superoxide dismutase inactivation in pathophysiology of asthmatic airway remodeling and reactivity. *Am J Pathol* 2005;166:664-74.
150. Dweik R, Comhair S, Gaston B, Thunnissen F, Farver C, Thomassen M, et al. NO chemical events in the human airway during the immediate and late antigen-induced asthmatic response. *Proc Natl Acad Sci U S A* 2001;98:2622-7.
151. Ghosh S, Janocha AJ, Aronica MA, Swaidani S, Comhair SA, Xu W, et al. Nitrotyrosine proteome survey in asthma identifies oxidative mechanism of catalase inactivation. *J Immunol* 2006;176:5587-97.
152. Postma D, Renkema T, Nordhoek J, Faber H, Sluiter H, Kaufman H. Association between nonspecific bronchial hyperreactivity and superoxide anion production

- by polymorphonuclear leukocytes in chronic air-flow obstruction. *Am Rev Respir Dis* 1988;137:57-61.
153. Saleh D, Ernst P, Lim S, Barnes P, Giaid A. Increased formation of the potent oxidant peroxyxynitrate in the airways of asthmatic patients is associated with induction of nitric oxide synthase: effect of inhaled glucocorticoid. *FASEB J* 1998;12:929-37.
  154. Sedgwick J, Calhoun W, Vrtis R, Bates M, McAllister P, Busse W. Comparison of airway and blood eosinophil function after in vivo antigen challenge. *J Immunol* 1992;149:3710-8.
  155. Zheng L, Nukuna B, Brennan M, Sun M, Goormastic M, Settle M, et al. Apolipoprotein A-I is a selective target for myeloperoxidase-catalyzed oxidation and functional impairment in subjects with cardiovascular disease. *J Clin Invest* 2004;114:529-41.
  156. Jarjour NN, Busse WW, Calhoun WJ. Enhanced production of oxygen radicals in nocturnal asthma. *Am Rev Respir Dis* 1992;146:905-11.
  157. Jarjour N, Calhoun W. Enhanced production of oxygen radicals in asthma. *J Lab Clin Med* 1994;123:131-6.
  158. Comhair S, Erzurum S. Redox control of asthma: molecular mechanisms and therapeutic opportunities. *Antioxid Redox Signal* 2010;12:93-124.
  159. De Raevae H, Thunnissen F, Kaneko F, Guo F, Lewis M, Kavuru M, et al. Decreased Cu,Zn-SOD activity in asthmatic airway epithelium: correction by inhaled corticosteroid in vivo. *Am J Physiol Lung Cell Mol Physiol* 1997;272:L148-54.
  160. MacNee W. Oxidative stress and lung inflammation in airways disease. *Eur J Pharmacol* 2001;429:195-207.
  161. Rahman I, MacNee W. Oxidative stress and regulation of glutathione in lung inflammation. *Eur Respir J* 2000;16:534-54.
  162. Jacquier-Sarlin M, Polla B, Slosman D. Oxido-reductive state: the major determinant for cellular retention of technetium-99m-HMPAO. *J Nucl Med* 1996;37:1413-6.
  163. Shih W, Rehm S, Grunwald F, Coupal J, Biersack H, Berger R, et al. Lung uptake of Tc-99m HMPAO in cigarette smokers expressed by lung/liver activity ratio. *Clin Nucl Med* 1993;18:227-30.
  164. Suga K, Uchisako H, Nishigauchi K, Shimizu K, Kume N, Yadama N, et al. Technetium-99m-HMPAO as a marker of chemical and irradiation lung injury: experimental and clinical investigations. *J Nucl Med* 1994;35:1520-7.
  165. Shaw T, Wakely S, Peebles C, Mehta R, Turner J, Wilson S, et al. Endobronchial ultrasound to assess airway wall thickening: validation in vitro and in vivo. *Eur Respir J* 2004;23:813-7.
  166. Soja J, Grzanka P, Sladek K, Okon K, Cmiel A, Mikos M, et al. The use of endobronchial ultrasonography in assessment of bronchial wall remodeling in patients with asthma. *Chest* 2009;136:797-804.
  167. Biernacki W, Redpath A, Best J, MacNee W. Measurement of CT lung density in patients with chronic asthma. *Eur Respir J* 1997;10:2455-9.
  168. Mitsunobu F, Ashida K, Hosaki Y, Tsugeno H, Okamoto M, Nishida N, et al. Decreased computed tomographic lung density during exacerbation of asthma. *Eur Respir J* 2003;22:106-12.
  169. Zeidler M, Goldin J, Kleerup E, Kim H, Truong D, Gjertson D, et al. Small airways response to naturalistic cat allergen exposure in subjects with asthma. *J Allergy Clin Immunol* 2006;118:1075-81.
  170. Ueda T, Niimi A, Matsumoto H, Takemura M, Hirai T, Yamaguchi M, et al. Role of small airways in asthma: investigation using high-resolution computed tomography. *J Allergy Clin Immunol* 2006;118:1019-25.
  171. Niimi A, Matsumoto H, Amitani R, Nakano Y, Mishima M, Minakuchi M, et al. Airway wall thickness in asthma assessed by computed tomography. Relation to Clinical Indices. *Am J Respir Crit Care Med* 2000;162:1518-23.
  172. Aysola R, Cook-Granroth J, Gierada D, Hoffman E, Wenzel S, Tarsi J, et al. Airway remodeling measured by multidetector CT is increased in severe asthma and correlates with pathology. *Chest* 2008;134:1183-91.
  173. Awadh N, Müller N, Park C. Airway wall thickness in patients with near fatal asthma and control groups: assessment with high resolution computed tomographic scanning. *Thorax* 1998;53:248-53.
  174. Little S, Sproule M, Cowan M, Macleod K, Robertson M, Love J, et al. High resolution computed tomographic assessment of airway wall thickness in chronic asthma: reproducibility and relationship with lung function and severity. *Thorax* 2002;57:247-53.
  175. Niimi A, Matsumoto H, Takemura M, Ueda T, Chin K, Mishima M. Relationship of airway wall thickness to airway sensitivity and airway reactivity in asthma. *Am J Respir Crit Care Med* 2003;168:983-8.
  176. Kasahara K, Shiba K, Ozawa T, Okuda K, Adachi M. Correlation between the bronchial subepithelial layer and whole airway wall thickness in patients with asthma. *Thorax* 2002;57:242-6.
  177. Matsumoto H, Niimi A, Takemura M, Ueda T, Minakuchi M, Tabuena R, et al. Relationship of airway wall thickening to an imbalance between matrix metalloproteinase-9 and its inhibitor in asthma. *Thorax* 2005;60:277-81.
  178. Tunon-de-Lara J, Laurent F, Giraud V, Perez T, Aguilaniu B, Meziane H, et al. Air trapping in mild and moderate asthma: effect of inhaled corticosteroids. *J Allergy Clin Immunol* 2007;119:583-90.
  179. Zeidler M, Kleerup E, Goldin J, Kim H, Truong D, Simmons M, et al. Montelukast improves regional air-trapping due to small airways obstruction in asthma. *Eur Respir J* 2006;27:307-15.
  180. Niimi A, Matsumoto H, Amitani R, Nakano Y, Sakai H, Takemura M, et al. Effect of short-term treatment with inhaled corticosteroid on airway wall thickening in asthma. *Am J Med* 2004;116:725-31.
  181. Haldar P, Brightling C, Hargadon B, Gupta S, Monteiro W, Sousa A, et al. Mepolizumab and exacerbations of refractory eosinophilic asthma. *N Engl J Med* 2009;360:973-84.
  182. Cox G, Laviolette M, Rubin A, Thomson N. Long term safety of bronchial thermoplasty (BT): 3 year data from multiple studies [abstract]. *Am J Respir Crit Care Med* 2009;179:A2780.
  183. Stoel B, Bode F, Rames A, Soliman S, Reiber J, Stolk J. Quality control in longitudinal studies with computed tomographic densitometry of the lungs. *Proc Am Thorac Soc* 2008;5:929-33.
  184. Stoel B, Putter H, Bakker M, Dirksen A, Stockley R, Piitulainen E, et al. Volume correction in computed tomography densitometry for followup studies on pulmonary emphysema. *Proc Am Thorac Soc* 2008;5:919-24.
  185. Mayo J. Radiation dose issues in longitudinal studies involving computed tomography. *Proc Am Thorac Soc* 2008;5:934-9.
  186. Smith-Bindman R, Lipson J, Marcus R, Kim K, Mahesh M, Gould R, et al. Radiation dose associated with common computed tomography examinations and the associated lifetime attributable risk of cancer. *Arch Intern Med* 2009;169:2078-86.
  187. Berrington de Gonzalez A, Mahesh M, Kim K, Bhargavan M, Lewis R, Mettler F, et al. Projected cancer risks from computed tomographic scans performed in the United States in 2007. *Arch Intern Med* 2009;169:2071-7.
  188. Einstein A, Henzlova M, Rajagopalan S. Estimating risk of cancer associated with radiation exposure from 64-slice computed tomography coronary angioplasty. *JAMA* 2007;298:317-23.